Supplementary Information

Particle diffusion in extracellular hydrogels

Federica Burla[1], Tatjana Sentjabrskaja[1], Galja Pletikapic[1], Joey van Beugen[1], Gijsje H. Koenderink[1,2,#]

[1] *AMOLF, Department of Living Matter, Biological Soft Matter group, Science Park 104, 1098 XG Amsterdam, the Netherlands*

[2] *Current address: Department of Bionanoscience, Kavli Institute of Nanoscience Delft, Delft University of Technology, Van der Maasweg 9, 2629 HZ Delft, the Netherlands*

[#] *Corresponding author: g.h.koenderink@tudelft.nl*

List of Supplementary Figures:

Figure S12: Evolution of the width and the non-Gaussian parameter ξ of the van Hove distribution functions with lag time, measured for tracer particles (0.6 μm) in 4 mg/mL hyaluronan networks with varied crosslinking conditions.

Figure S13: Microrheology analysis of DDM data for collagen-only network at 1 and 2 mg/mL, semidiluted hyaluronan at 2 mg/mL and for collagen (1 mg/ml)/hyaluronan (2 mg/ml) composite with 0.6 μm particles.

Figure S14: Transport coefficients *K* and subdiffusive exponents α from DDM and from particle tracking for tracer particles (0.6 μm) in 1 mg/mL and 2 mg/mL collagen, 2 mg/mL semidiluted hyaluronan, and composite 1 mg/mL collagen- 2 mg/mL hyaluronan networks.

Figure S15: Evolution of exponential tails of the van Hove distributions of collagen-only network at 1 mg/mL, semidiluted hyaluronan at 2 mg/mL and for collagen-hyaluronan composite at 1 mg/mL collagen-2 mg/mL hyaluronan with 0.6 μm particles probe size.

Figure S16: Non-Gaussian parameter ξ characterizing van Hove distribution functions for collagen-only network at 1 and 2 mg/mL, hyaluronan at 2 mg/mL and for collagen (1 mg/ml)/hyaluronan (2 mg/ml) composite with 0.6 μm particles.

Figure S17: Degree of heterogeneity in particle dynamics across ROIs for collagen-only networks and for collagen-hyaluronan composites.

Figure S18: ISF from DDM and van Hove distribution from particle tracking for a collagen-only network at a concentration of 2 mg/mL.

Figure S19: Linear rheology of 1 and 2 mg/mL collagen-only and composite 1 mg/mL collagen-2 mg/mL hyaluronan networks.

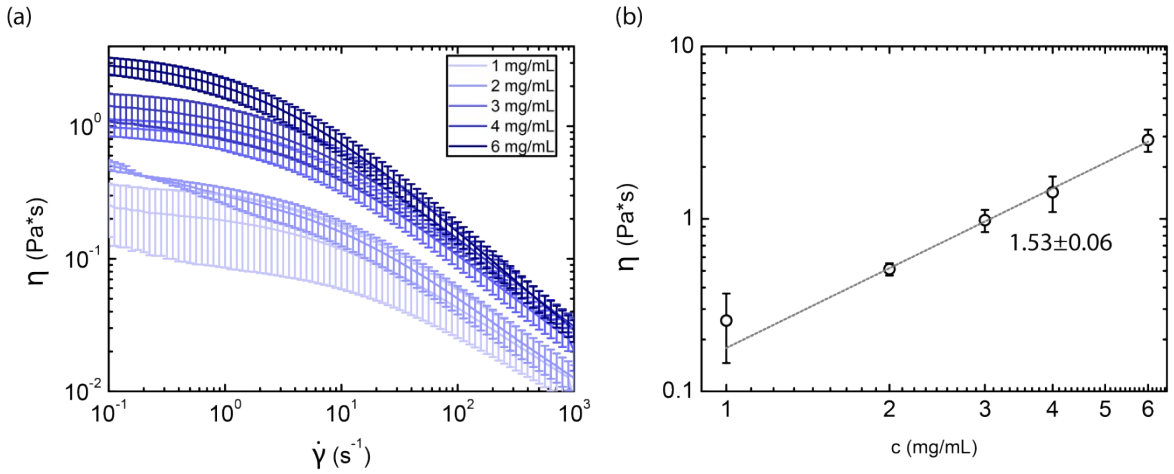

Supplementary Figure S1: Concentration dependence of the shear viscosity of semidilute hyaluronan solutions. (a) Shear viscosity as a function of shear rate for semidilute hyaluronan solutions with concentrations from 1 mg/mL to 6 mg/mL (see legend) determined with shear rheometry. (b) The low-shear viscosity (reported for $\dot{\gamma} = 0.1\ s^{-1}$) scales with concentration c with a power law relationship $\eta = ac^b$, where b is 1.53±0.06. This exponent is roughly consistent with the expected b≈1.3 scaling of semidilute polymer solutions. The data represents an average over three independent measurements and the error reported is the standard error of the mean.

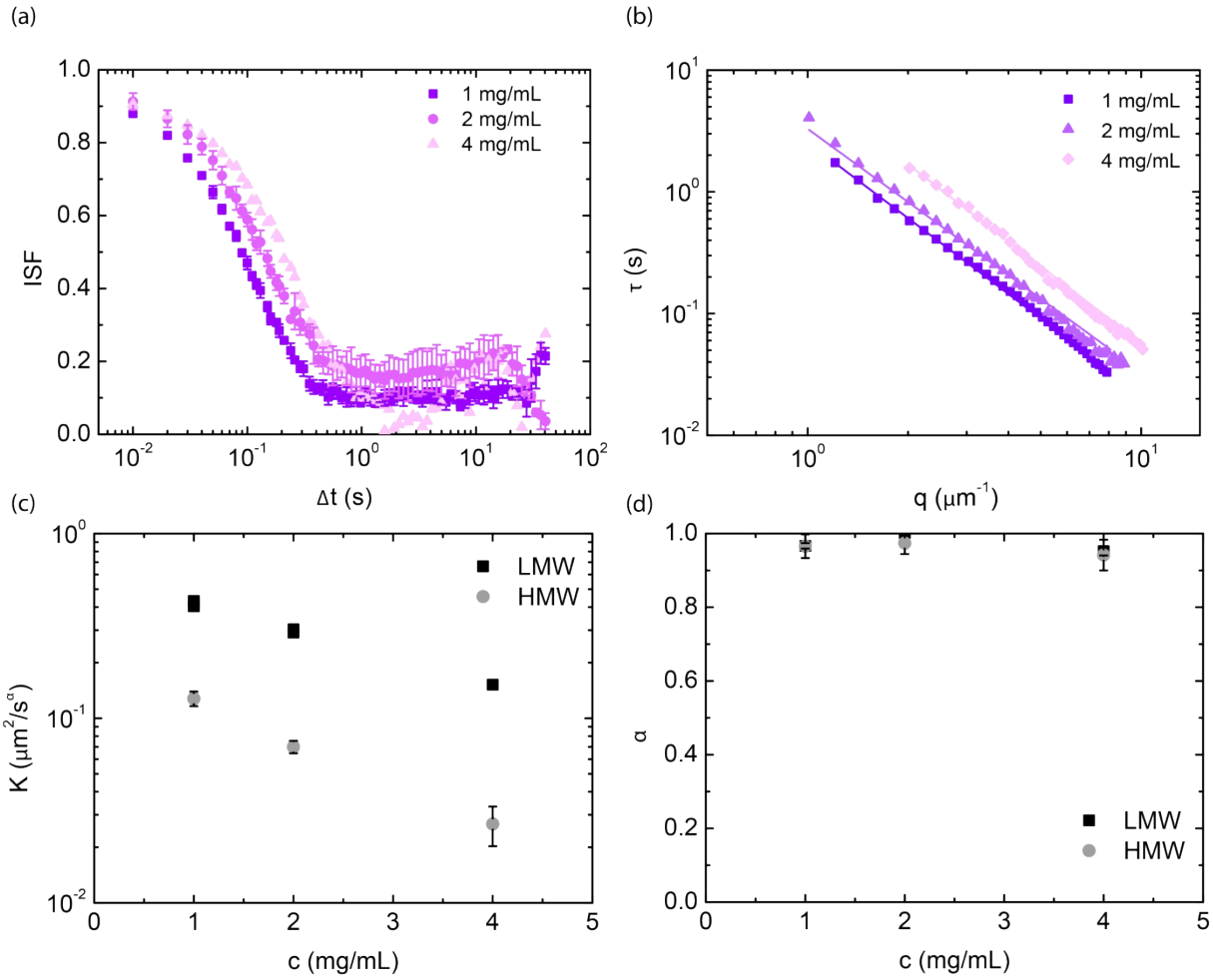

Supplementary Figure S2: DDM measurements of semidilute hyaluronan solutions, comparing high (240 kDa) and low (1.5 MDa) molecular weight samples for 0.6 µm particles. (a) ISF for hyaluronan of low molecular weight (240 kDa) at different concentrations, without chemical crosslinking. (b) τ(q) for the same samples. (c) Comparison of transport coefficient *K* and (d) subdiffusive exponent α for high molecular weight (HMW) and low molecular weight (LMW) samples.

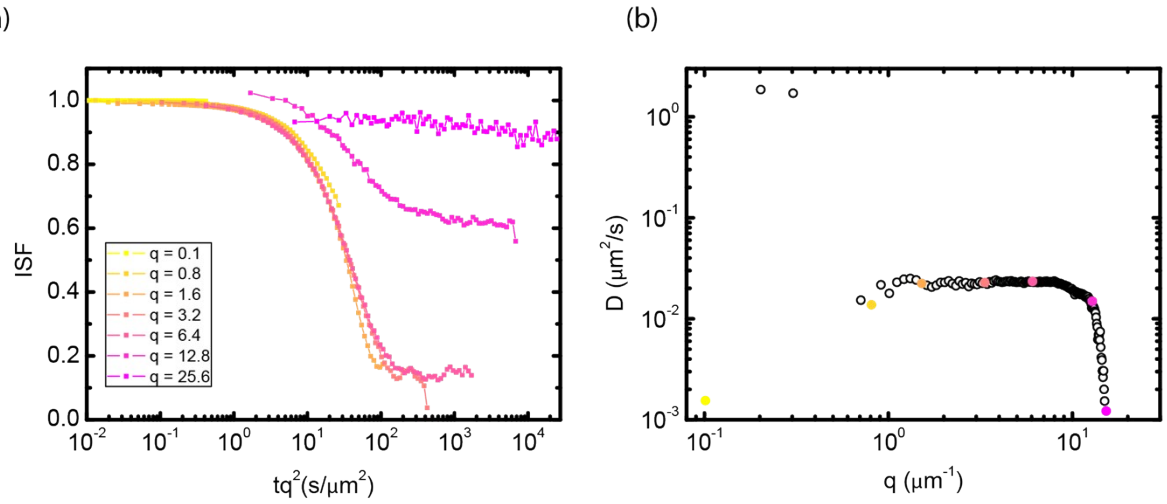

Supplementary Figure S3: Wavevector dependence of the intermediate scattering function (ISF). (a) ISF for 0.6 µm tracer particles embedded in 4 mg/mL (semidilute) hyaluronan solutions. Different colours indicate different *q*-values (expressed in the legend in units of µm^{-1}). For low *q*-values (0.1 µm^{-1}), the ISF does not fully decorrelate, because the measurement spans the whole field of view. At high *q*-values (≥12.8 µm^{-1}), the measurement is dominated by noise because of the drifting of particles outside the field of view. (b) Apparent diffusion coefficient obtained from stretched exponential fits of the ISFs as a function of *q*, with colored symbols corresponding to the corresponding curves in panel a.

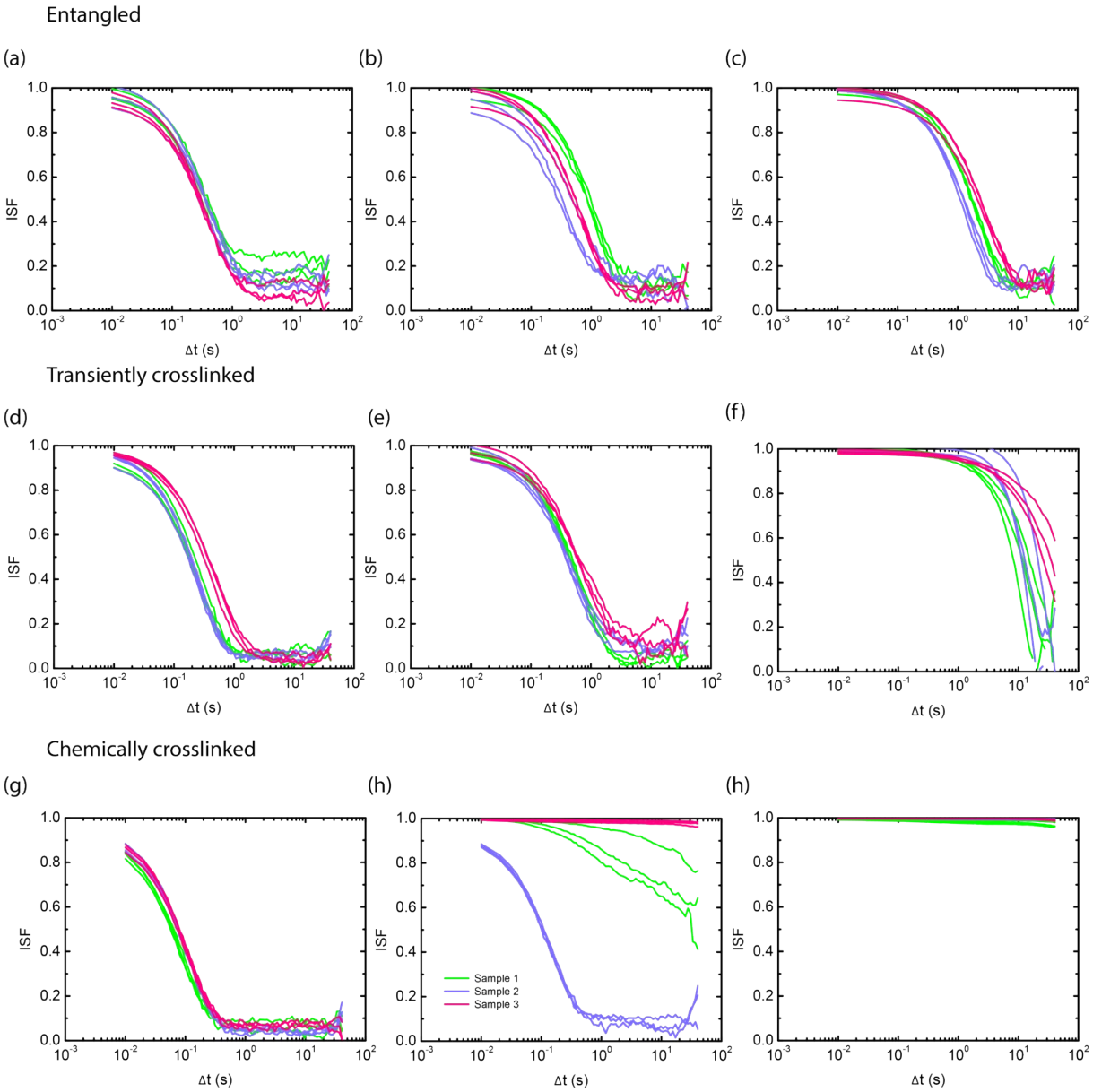

Supplementary Figure S4: Degree of heterogeneity in particle dynamics among ROIs for hyaluronan-only samples for different hyaluronan concentrations and crosslinking states (with 0.6 µm tracer particles). (a-b-c) ISF at q=4.5 μm^{-1} for semidilute samples, transiently crosslinked samples (d-e-f) and chemically crosslinked samples (g-h-i) at hyaluronan concentrations of 1 mg/mL (left column), 2 mg/mL (central column) and 4 mg/mL (right column). Each color represents an independently prepared sample, and each line represents data from one region of interest.

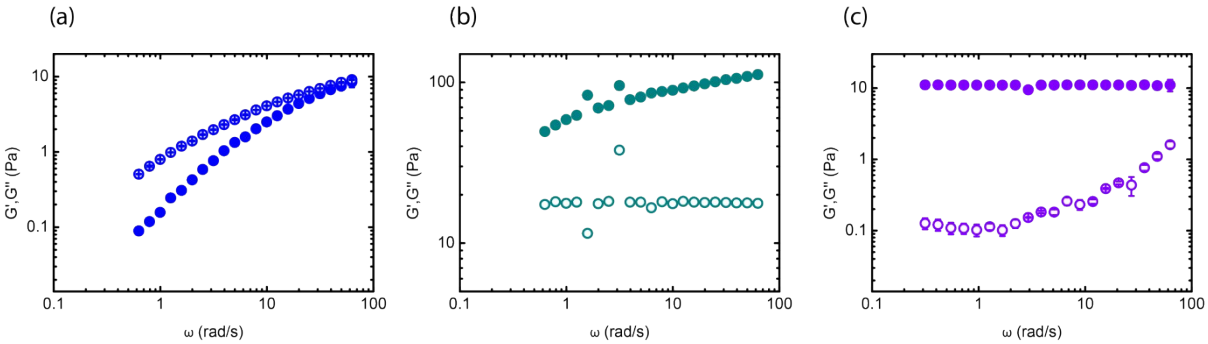

Supplementary Figure S5: Bulk rheology of the hyaluronan solutions and gels in the linear viscoelastic regime. (a) Frequency sweep of a semidilute hyaluronan solution at 4 mg/mL, which shows predominantly viscous behavior. (b) Frequency sweep of a transiently crosslinked hyaluronan gel (pH 2.5, putty state) at 4 mg/mL, which behaves as a transient gel. (c) Frequency sweep of a covalently crosslinked hyaluronan gel at 4 mg/mL, which behaves as a soft solid. The results are shown as an average of three repeats over independently prepared samples. The error bar represents the standard error of the mean. Full circles indicate elastic shear moduli *G*' and empty circles indicate loss shear moduli *G*''.

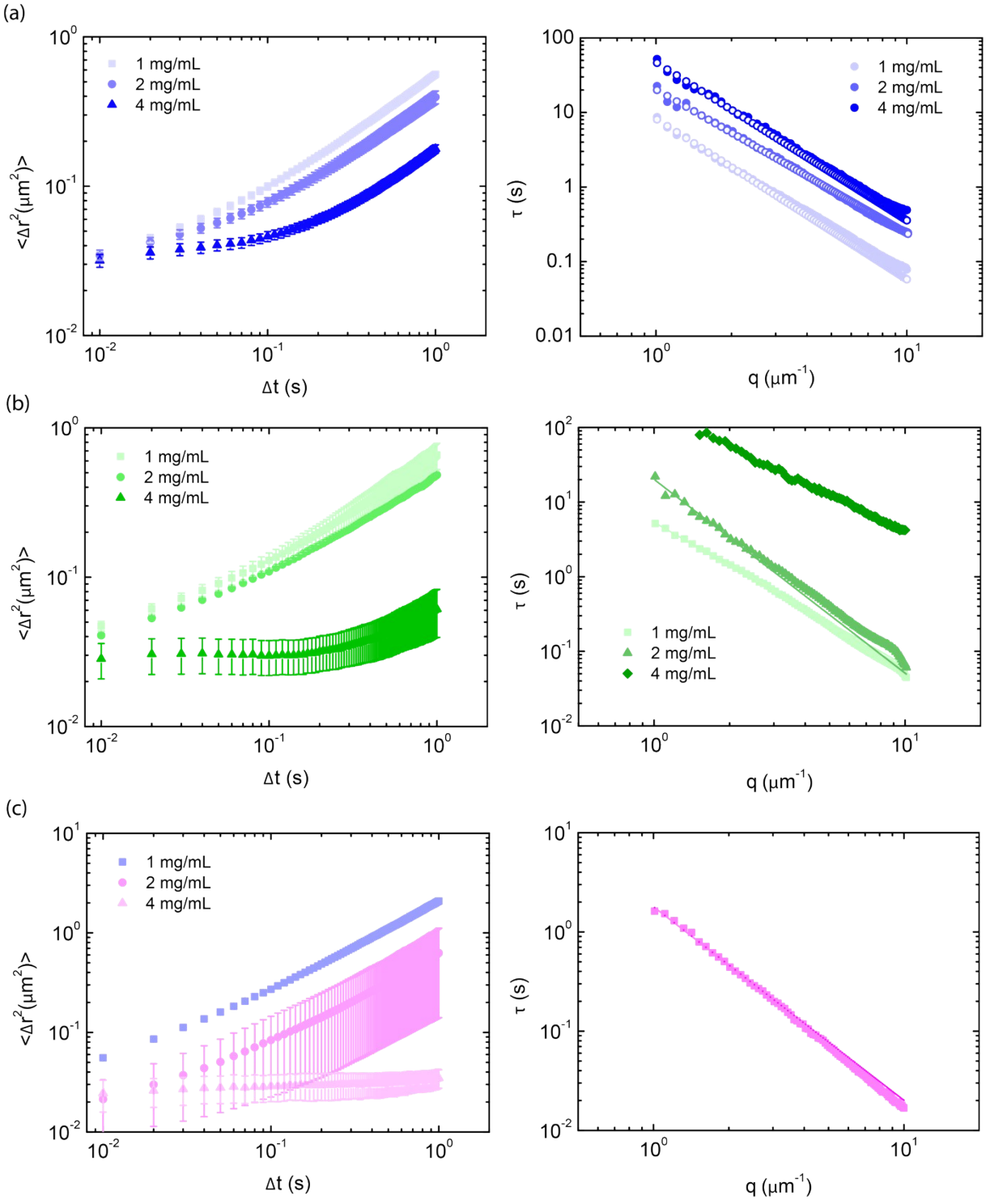

Supplementary Figure S6: MSD from single particle tracking and τ(q) from DDM for different hyaluronan concentrations and crosslinking states measured with 0.6 µm particles. Left panels: MSD determined from single-particle tracking for (a) entangled, (b) transiently crosslinked and (c) chemically crosslinked networks at concentrations between 1 and 4 mg/mL. Right panels: relaxation time τ obtained from fitting ISFs to a stretched exponential, for different values of q. In the crosslinked case, we show only the value of τ at 1 mg/mL because the results at 2 mg/mL and 4 mg/mL do not show a full relaxation for the ISF.

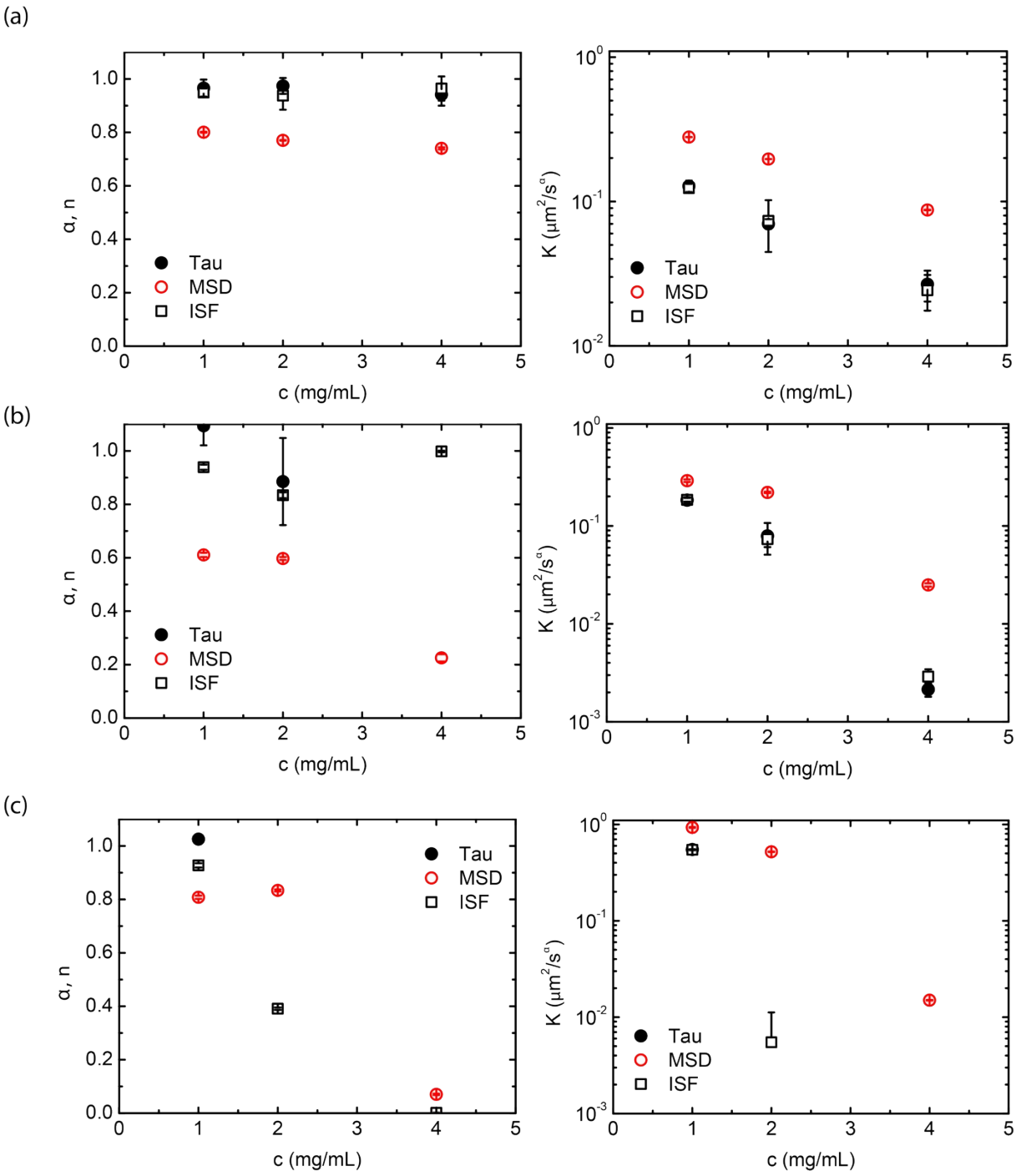

Supplementary Figure S7: Subdiffusive exponents α and transport coefficients *K* determined from fitting τ(q), the decay of the ISF, and the lag time dependence of the MSD from particle tracking, for different hyaluronan concentrations and crosslinking states and for 0.6 μm particles. Results show the subdiffusive exponent α or stretching exponent *n* (left panel) and transport coefficient *K* (right panel) for semidilute (a), transiently crosslinked (b) and chemically crosslinked (c) networks. In all cases, the subdiffusive exponents obtained from MSD are below the values obtained from DDM. This is likely related to the short time-interval over which the MSD traces could be obtained.

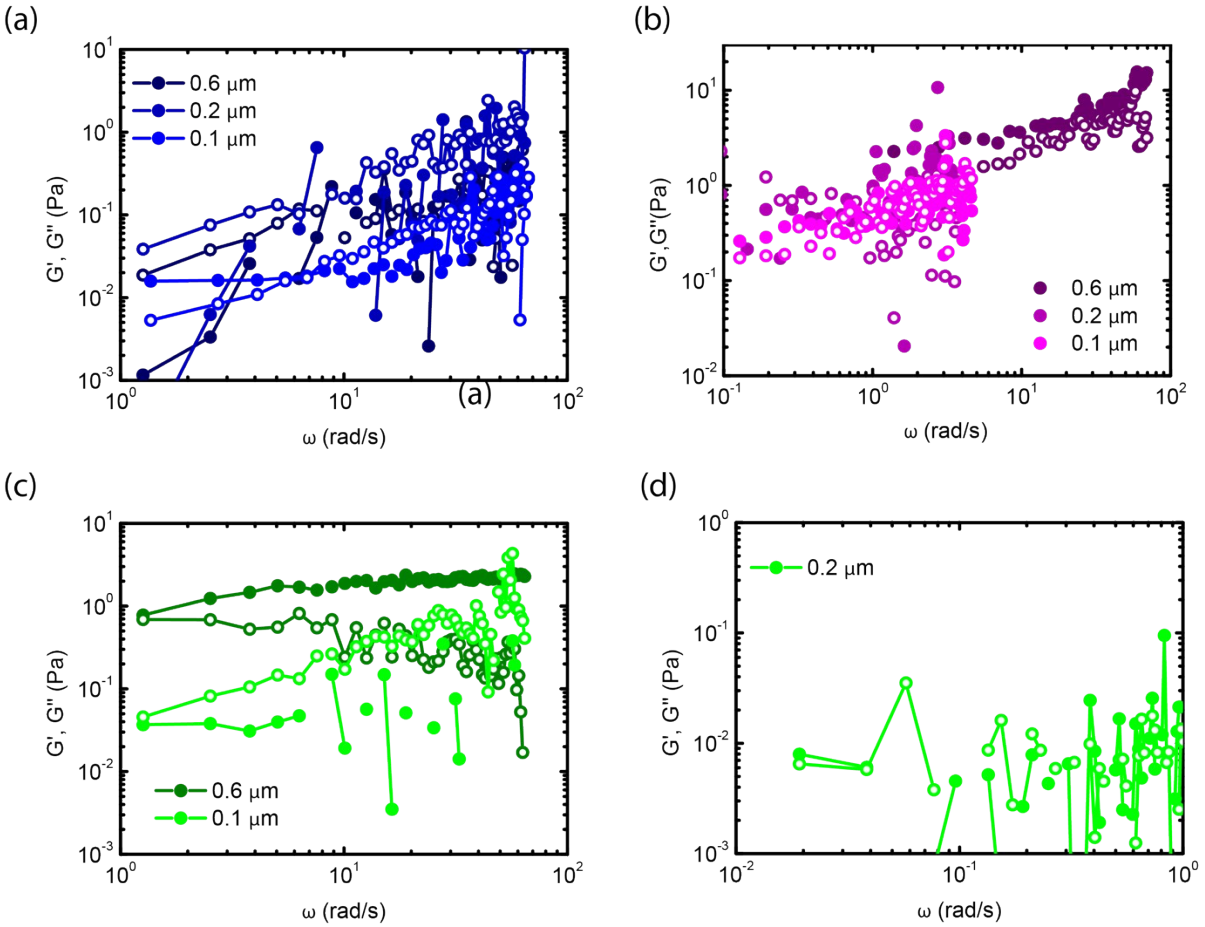

Supplementary Figure S8: Microrheology of hyaluronan gels at 4 mg/mL from DDM data probed with 0.1 μm, 0.2 μm and 0.6 μm particles. Microrheology storage and loss moduli for (a) semidilute, (b) permanently crosslinked and (c) transiently crosslinked hyaluronan networks obtained for different particle sizes, obtained from applying the Evans-Tassieri analysis method to the mean-squared-displacement obtained from DDM. Panel (d) represents microrheology of transiently crosslinked networks at a probe particle size of 0.2 μm. Solid circles represent the storage moduli G', and empty circles the loss moduli G''.

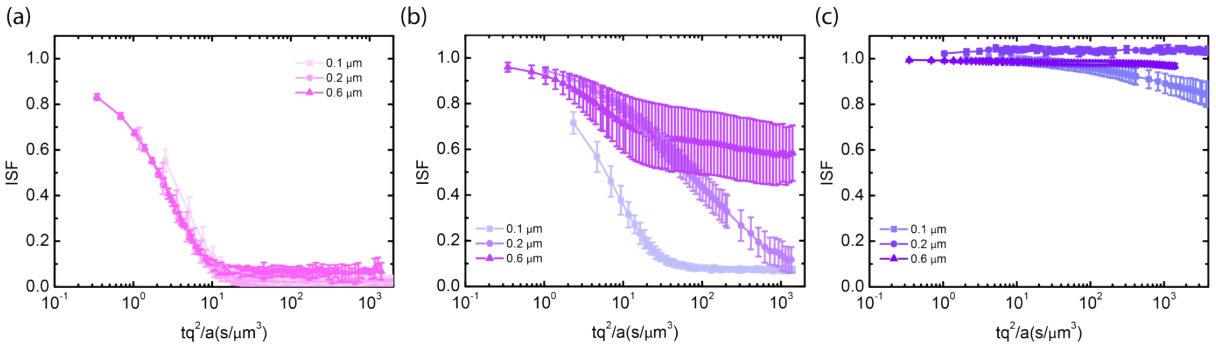

Supplementary Figure S9: Rescaling of the intermediate scattering function considering the particle size in crosslinked hyaluronan networks. (a) Collapse of the ISF of a 1 mg/mL crosslinked hyaluronan network for different particle sizes (see legend), obtained by dividing the x-axes for the particle diameter a. (b) Same rescaling for a 2 mg/mL and (c) a 4 mg/mL crosslinked hyaluronan network. Here, the size dependence of the diffusivity deviates from Stokes-Einstein behavior.

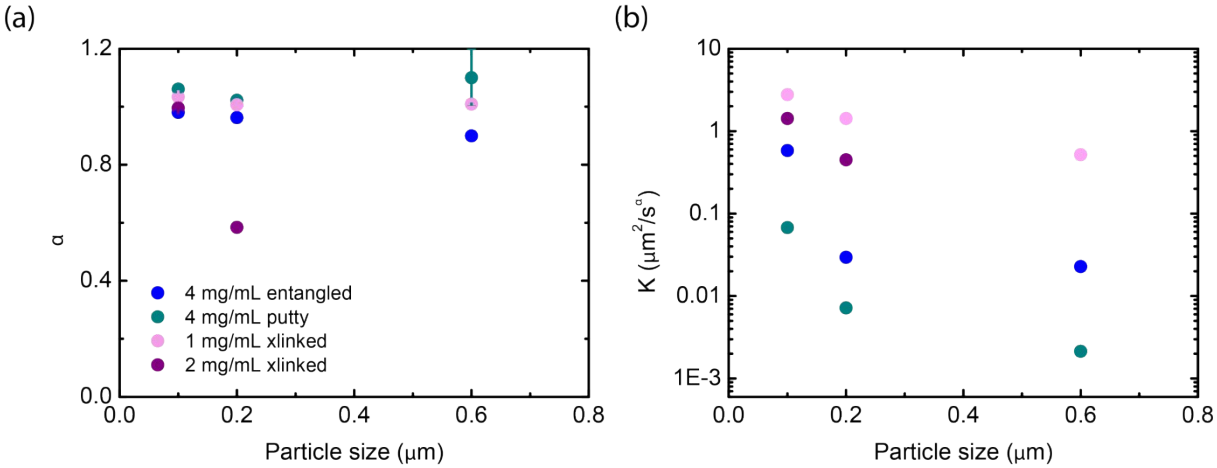

Supplementary Figure S10: Subdiffusive exponents α and transport coefficients *K* determined from DDM intermediate scattering functions for tracer particles of different sizes in variously crosslinked hyaluronan networks. (a) Subdiffusive exponent for different hyaluronan gels (see Legend) as a function of tracer particle diameter, obtained from fitting the decay of τ (q). (b) Transport coefficient for different hyaluronan gels as a function of tracer particle diameter. Values represent averages over at least 9 measurements obtained over three independently prepared samples, and the error shown is the standard error of the mean. For the crosslinked networks, we could not analyze data obtained at 4 mg/mL hyaluronan because of the incomplete decay of the ISF.

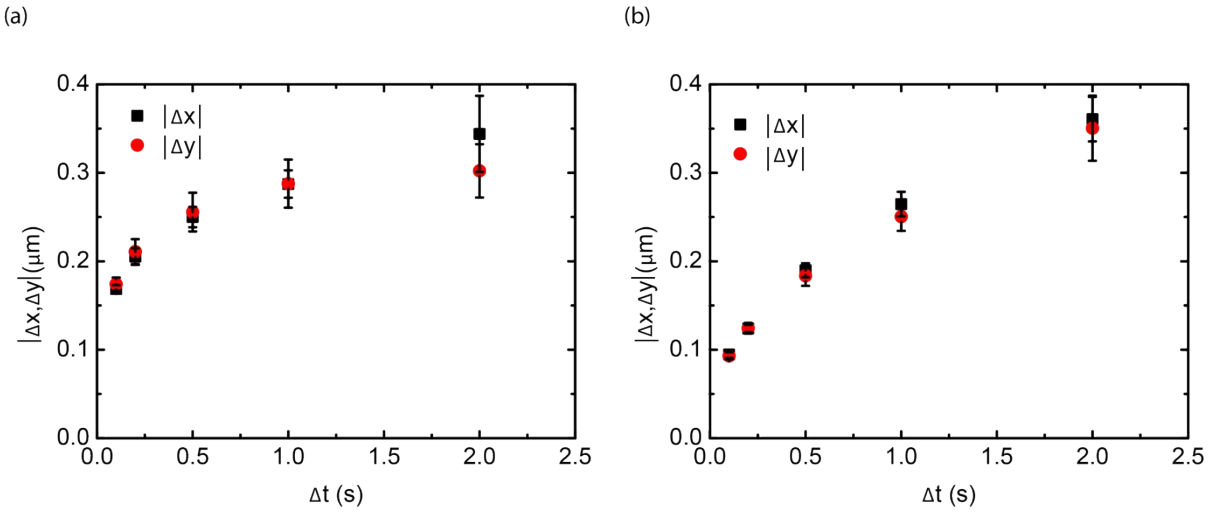

Supplementary Figure S11: Isotropy in x-y displacements for two representative examples of 4 mg/mL semidilute hyaluronan and 2 mg/mL collagen for 0.6 μm particles. Representative examples are shown for a (a) collagen-only network at 2 mg/mL and (b) an entangled hyaluronan network at 4 mg/mL for different lag times.

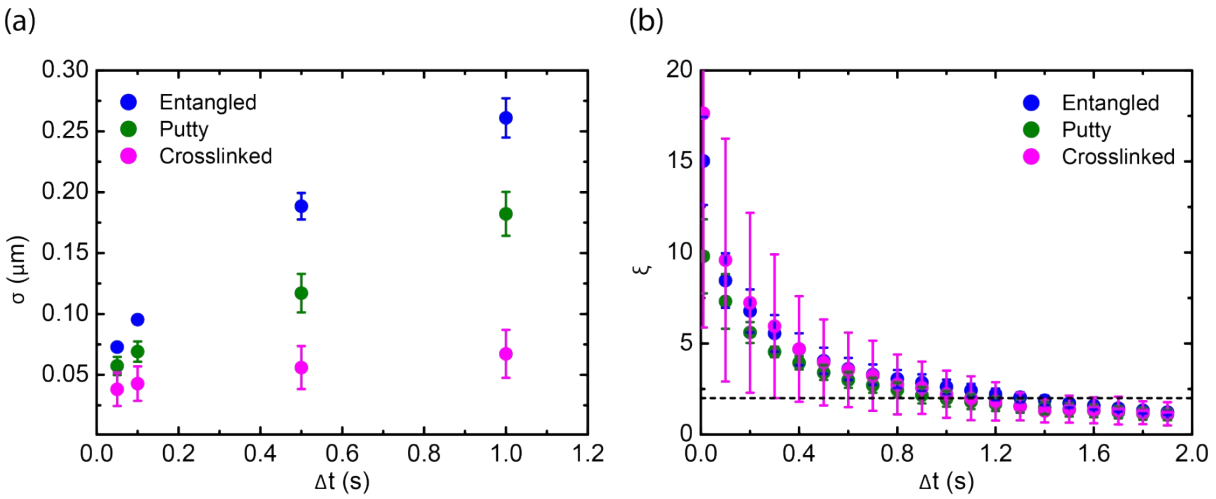

Supplementary Figure S12: Evolution of the width and the non-Gaussian parameter *ξ* of the van Hove distribution functions with lag time, measured for tracer particles (0.6 μm) in hyaluronan networks with varied crosslinking conditions. (a) The width was obtained from fitting the van Hove distributions to a Gaussian function for semidilute solutions (blue), transiently crosslinked gels (green), and chemically crosslinked gels (purple) of hyaluronan (all at 4 mg/ml). Data represents an average over three independent measurements and the errors shown represent the standard error of the mean (b) Non-gaussian parameter calculated as a function of lag time for entangled (blue), transiently crosslinked (green) and chemically crosslinked (pink) samples. The dotted line represents the expected value for an exponential distribution (ξ =2). The monotonic decrease of *ξ* with lag-time reflects the fact that the displacements are initially smaller than the tracking accuracy (0.1 μm).

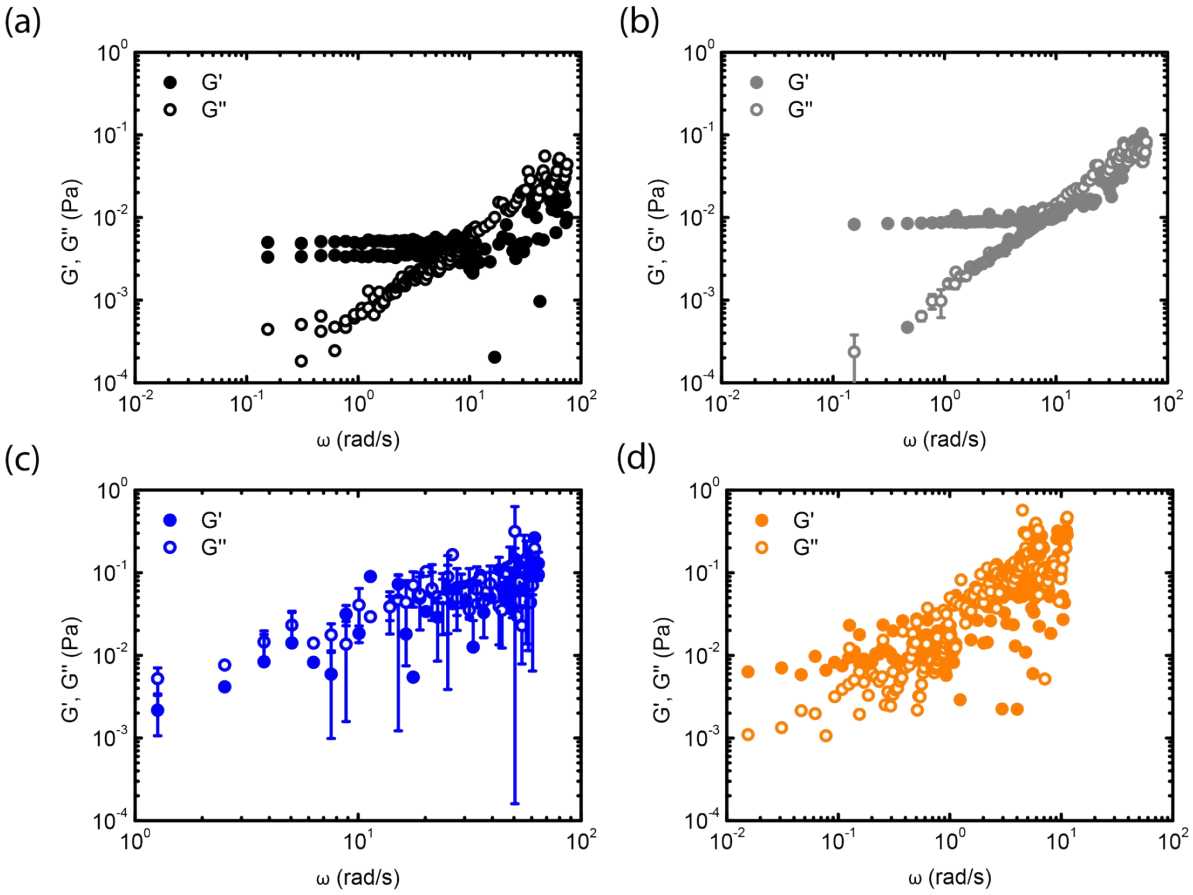

Supplementary Figure S13: Microrheology analysis of DDM data for collagen-only network at 1 and 2 mg/mL, semidilute hyaluronan at 2 mg/mL, and collagen (1 mg/mL)/hyaluronan (2 mg/mL) composite networks with 0.6 µm particles. (a) Microrheology for 1 mg/mL collagen, (b) 2 mg/mL collagen, (c) 2 mg/mL pure hyaluronan and (d) composite composed of 2 mg/mL hyaluronan and 1 mg/mL collagen.

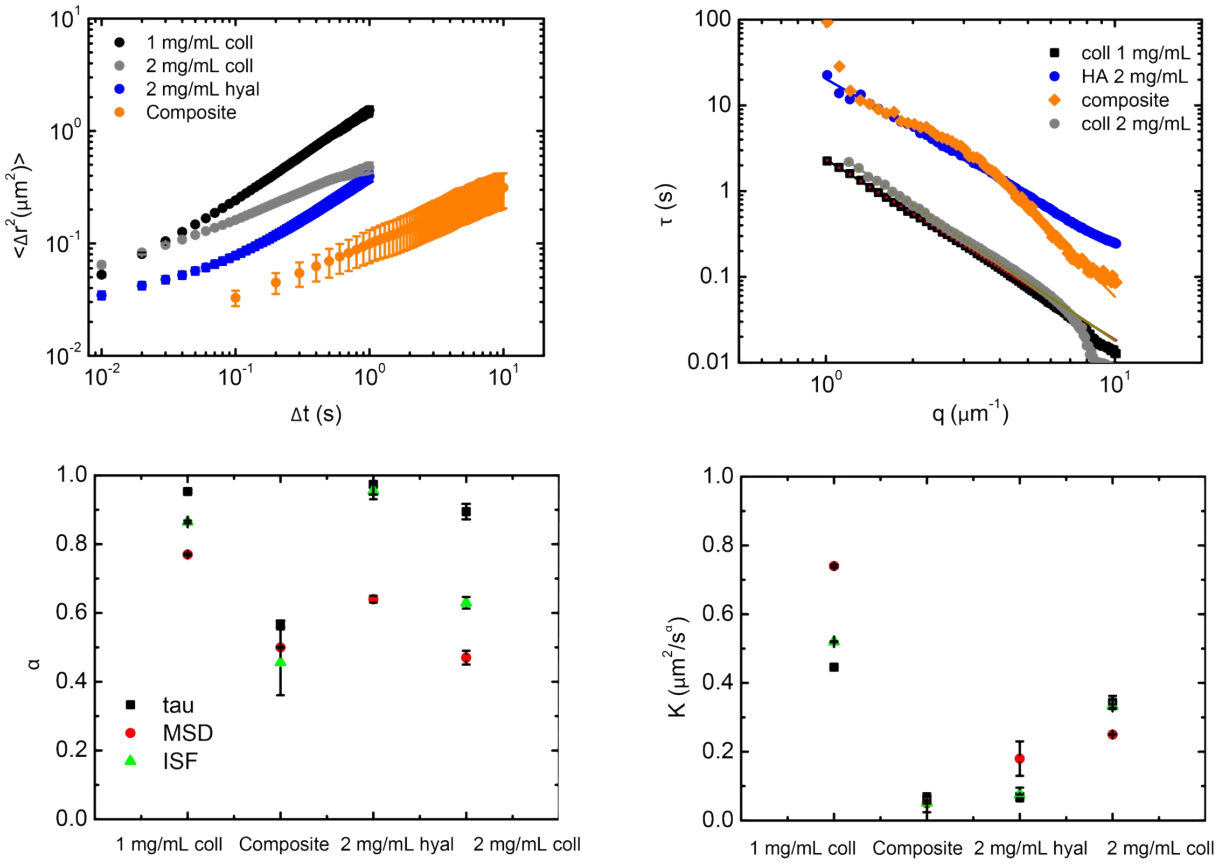

Supplementary Figure S14: Transport coefficients *K* and subdiffusion exponents α from DDM and from particle tracking for tracer particles (0.6 µm) in 1 mg/mL and 2 mg/mL collagen, 2 mg/mL semidiluted hyaluronan, and composite 1 mg/mL collagen- 2 mg/mL hyaluronan networks. (a) MSD from particle tracking, (b) $\tau(q)$ from DDM for composite networks of 1 mg/mL collagen and 2 mg/mL hyaluronan, for collagen-only networks (either 1 or 2 mg/ml), and for 2 mg/mL hyaluronan networks, and (c) subdiffusive exponents and (d) transport coefficients obtained for the same networks.

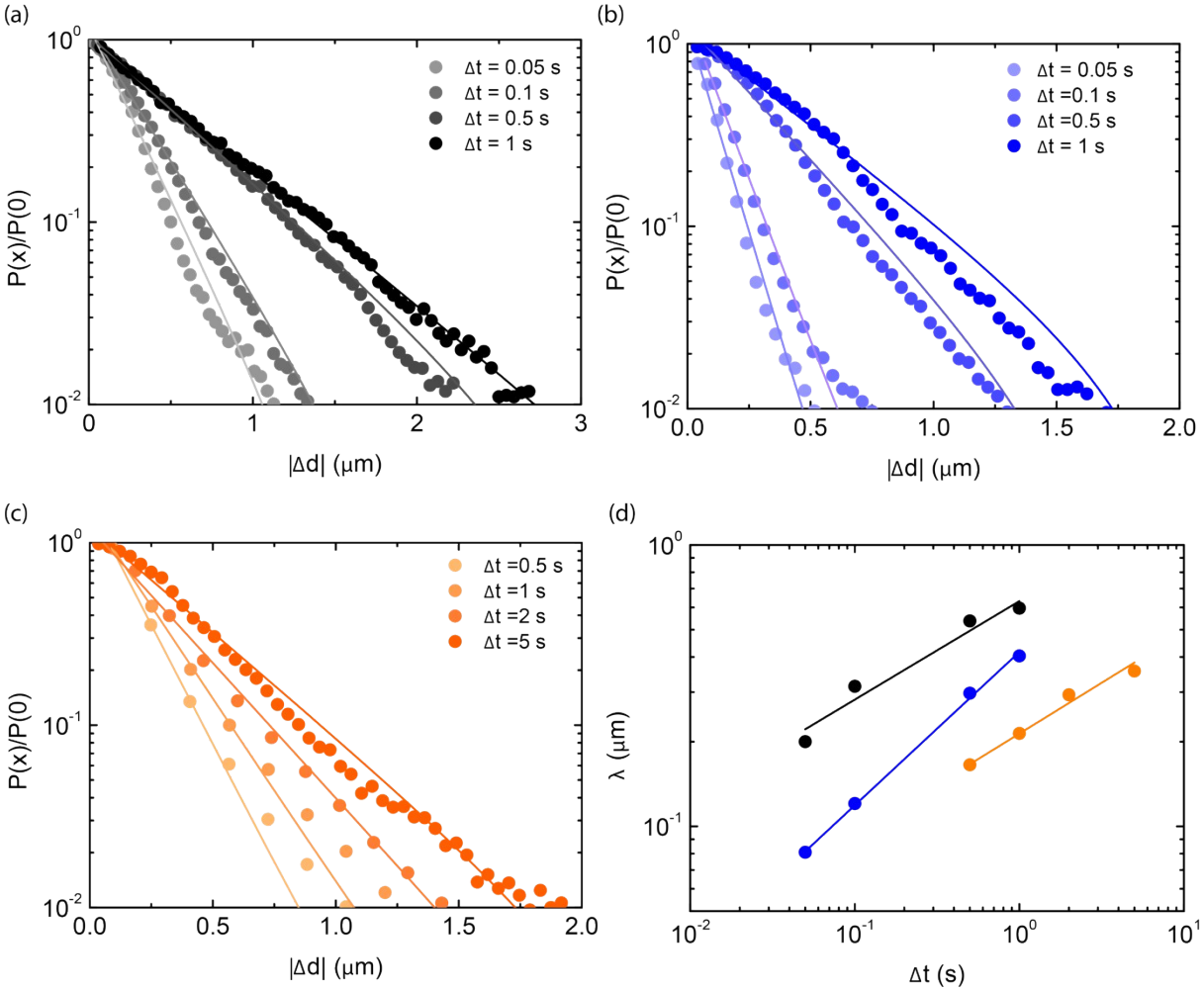

Supplementary Figure S15: Evolution of exponential tails of the van Hove distributions of collagen-only network at 1 mg/mL, semidiluted hyaluronan at 2 mg/mL and collagen-hyaluronan composite at 1 mg/mL collagen- 2 mg/mL hyaluronan with 0.6 μm particles probe size. Exponential decay for the van Hove distribution of (a) 1 mg/mL collagen networks, (b) 2 mg/mL hyaluronan solution and (c) 1 mg/mL collagen-2 mg/mL hyaluronan network. (d) Evolution of the decay exponent λ a as a function of lag time. Lines represent fits with power law slopes of: 0.35 ± 0.05 (collagen, black), 0.54 ±0.01 (hyaluronan, blue), 0.36 ± 0.03 (composite, orange). The error represents the error from the fit and the data points are obtained by pooling together all of the distributions of the data points for at least three different samples and over at least three different ROIs.

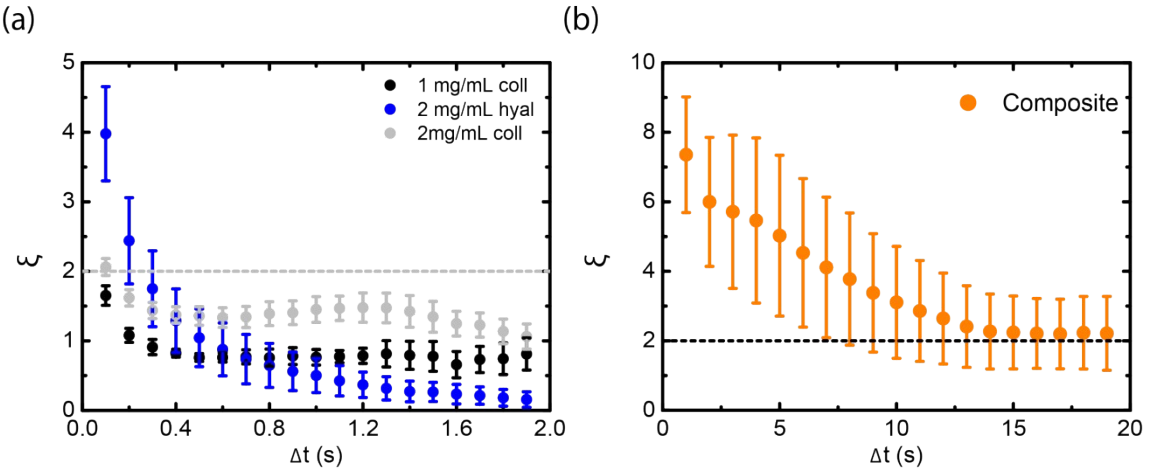

Supplementary Figure S16: Non-Gaussian parameter *ξ* characterizing van Hove distribution functions for collagen-only network at 1 and 2 mg/mL, hyaluronan at 2 mg/mL and for collagen (1 mg/ml)/hyaluronan (2 mg/ml) composite with 0.6 µm particles. (a) Non-Gaussian parameter calculated as a function of lag time for collagen (black), hyaluronan (blue) and composite (orange) samples. The dashed lines indicate the calculated value of *ξ* for an exponential distribution. The different timescales are related to the different acquisition times used for the samples.

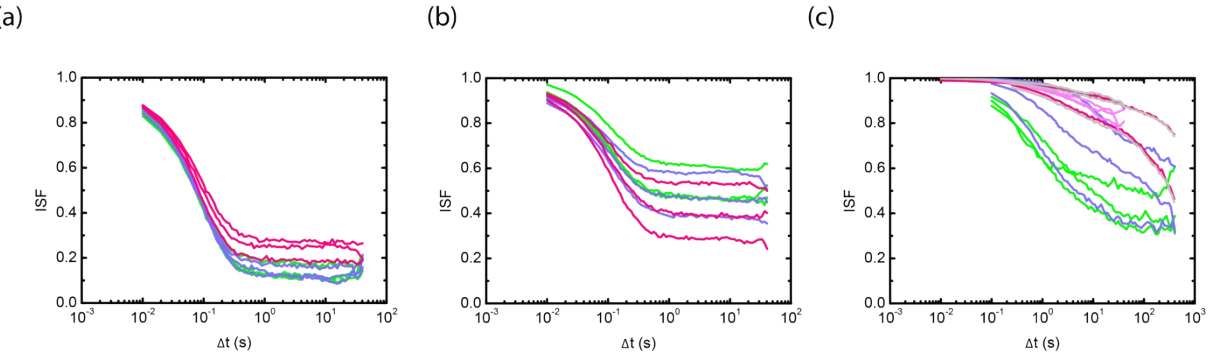

Supplementary Figure S17: Degree of heterogeneity in particle dynamics across ROIs for collagen-only networks and for collagen-hyaluronan composites. (a) ISF obtained for q = 4.5 µm^{-1} for (a) 1 mg/mL pure collagen network, (b) 2 mg/mL collagen-only network, and (c) a composite of 1 mg/mL collagen and 2 mg/mL hyaluronan. Each color represents an independently prepared sample, and each line represents one ROI.

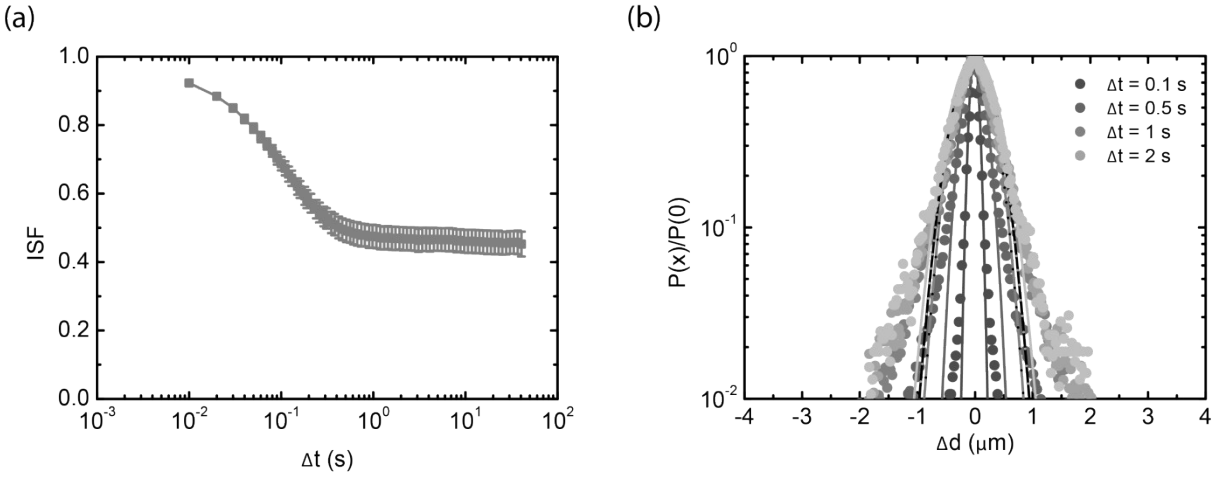

Supplementary Figure S18: ISF from DDM and van Hove distribution from particle tracking for a collagen-only network at a concentration of 2 mg/mL. (a) ISF at q= 4.5 μm^{-1} and (b) van Hove distribution at different lag times.

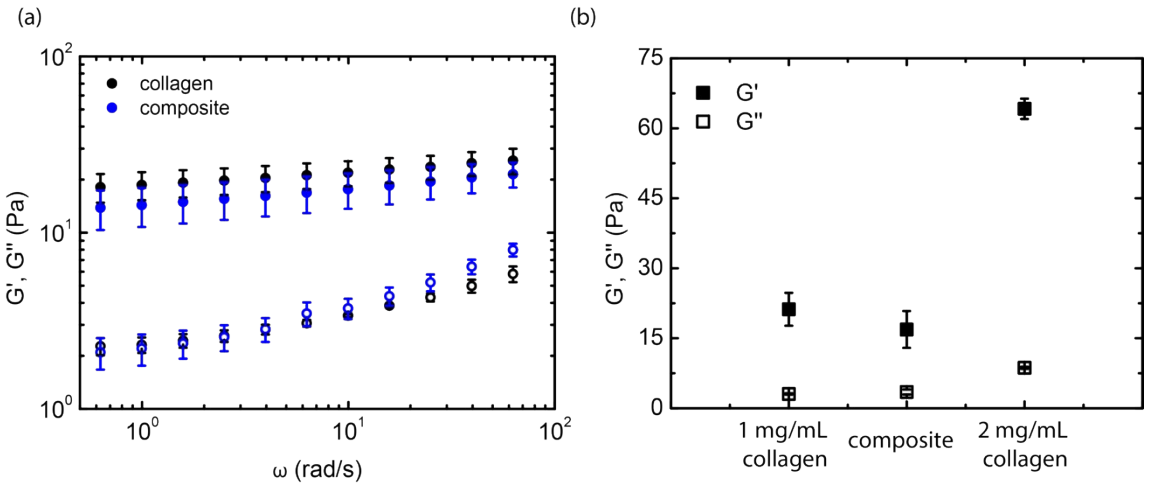

Supplementary Figure S19: Linear rheology of 1 and 2 mg/mL collagen-only and composite 1 mg/mL collagen-2 mg/mL hyaluronan networks. (a) Frequency sweep for a collagen network at 1 mg/mL (black symbols) and a composite collagen-hyaluronan network (1 and 2 mg/mL, respectively, blue symbols). The measurement represents an average over at least three different repeats, and the standard deviation represents the standard error of the mean. (b) Elastic (full symbols) and viscous (empty symbols) moduli for collagen networks at 1 and 2 mg/mL and composite networks with 1 mg/mL collagen and 2 mg/mL hyaluronan, measured at a frequency of 6.28 rad/s.